

Chapter

Direct Contact Heat and Mass Exchanger for Heating, Cooling, Humidification, and Dehumidification

*Marip Kum Ja, Qian Chen, Muhammad Burhan,
Doskhan Ybyraiymkul, Muhammad Wakil Shahzad,
Raid Alrowais and Kim Choon Ng*

Abstract

A direct-contact heat and mass exchanger (DCHME) has many advantages over a traditional surface-type heat exchanger, including a high heat transfer coefficient, simplicity of design, and low OPEX and CAPEX. DCHME has a capability to exchange of both heat and mass between the two fluids in the same process. Hence, DCHMEs are widely used in numerous applications in various industries, including the air conditioning industry for cooling and dehumidification and heating and humidification. Based on their structure, DCHME can be categorized into two groups; two fluids direct contact (TFDC) exchanger and two direct contacts with one non-contact fluid (TDCONF) exchanger. This study developed a mathematical model for these two types of exchangers by using a discretized volume with distributed lumped-parameters method instead of using the conventional log mean enthalpy difference (LMHD) and NTU-effectiveness method. Thus, this model can reflect both heat and mass transfer behavior in every spatially distributed physical system. The objective of this study is to develop a mathematical model to be used as a tool for designing DCHME and to be applied as a sub-function of the model predictive control system to predict the effectiveness and dependent parameters of DCHME under the different load conditions and its various input parameters.

Keywords: heat and mass exchanger, distributed lump model, humidification and dehumidification

1. Introduction

For more than 100 years ago, direct contact heat and mass exchangers (DCHME) have been widely used in various industries, including chemical process plant, food, and beverage industry, geothermal heat recovery, seawater desalination, waste heat recovery, energy storage systems, production of steam generation for the Rankine power cycle, air conditioning and refrigeration industries, and many so forth. DCHME is a device in which the two process streams are flowing and contacting each other to exchange heat and mass between these two streams,

which can be gas-solid, gas-liquid, liquid-liquid, liquid-solid, or solid-solid streams. The limitation of DCHME is the contamination of the streams depending on the degree of miscibility. Although it has a limitation, there are many advantages such as no corrode or foul or no degradation of heat transfer performance due to the lack of surfaces, a larger heat transfer surface area, much lower flow resistance compared with surface-type heat exchangers, and less capital and operational cost [1]. Thus, DCHMEs are widely used in air conditioning industry for cooling, heating and humidification, cooling and dehumidification, and cooling and humidification, such devices are swamp cooler or direct contact evaporative cooler, cooling tower, air washer spray chamber, cooling coil of air handling unit (AHU), direct expansion (DX) evaporator coil, indirect evaporative cooler, and M-cycle dew point evaporative cooler. Before developing the numerical model of these devices, the process of each device has required to analysis with the psychrometric chart. There are total of eight basic air conditioning processes, which are plotted on a psychrometric chart as shown in **Figure 1**. These processes are the air stream from the initial state O to the state (1) for sensible cooling, (2) for cooling and humidification, (3) for humidification only, (4) for heating and humidification, (5) for sensible heating, (6) for heating and dehumidification, (7) for dehumidification only, and (8) for cooling and dehumidification. In order to achieve the above eight processes, some processes need to transfer heat (sensible heat) only but some need to exchange heat and mass (sensible and latent heat) from the air stream. Process 1, cooling, and process 5, heating, are pure heat transfer processes only, which means removing heat from the air stream for cooling and adding heat to the air stream for heating without changing the moisture of the airflow. Process 3, humidification, and process 7, dehumidification, are pure mass transfer processes without variation in air temperature. The rest processes 2 (cooling and humidification), process 4 (heating and humidification), process 6 (heating and dehumidification), and process 8 (cooling and dehumidification) are both heat and mass (sensible and latent heat) transfer process that is adding or removing of heat and moisture to or from the air stream. For DCHME has a capability to transfer both heat and mass in the same process, almost all the processes except six can be accomplished by using DCHME in a single stage. The typical five DCHMEs mentioned above extensively used in the air conditioning industry are discussed with their basic air conditioning process.

(1) Swamp cooler or direct contact evaporative cooler, shown in **Figure 2(a)**, is a device in which the outside air flows through the medium of cooling pad or fill

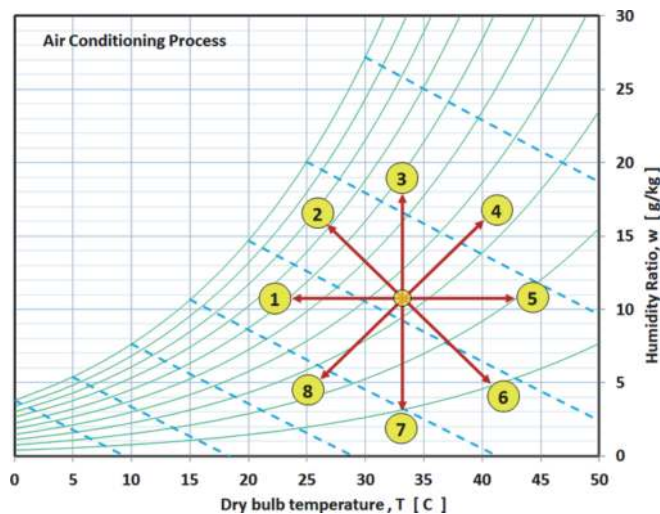


Figure 1.
Basic eight air conditioning processes plotted on the psychrometric chart.

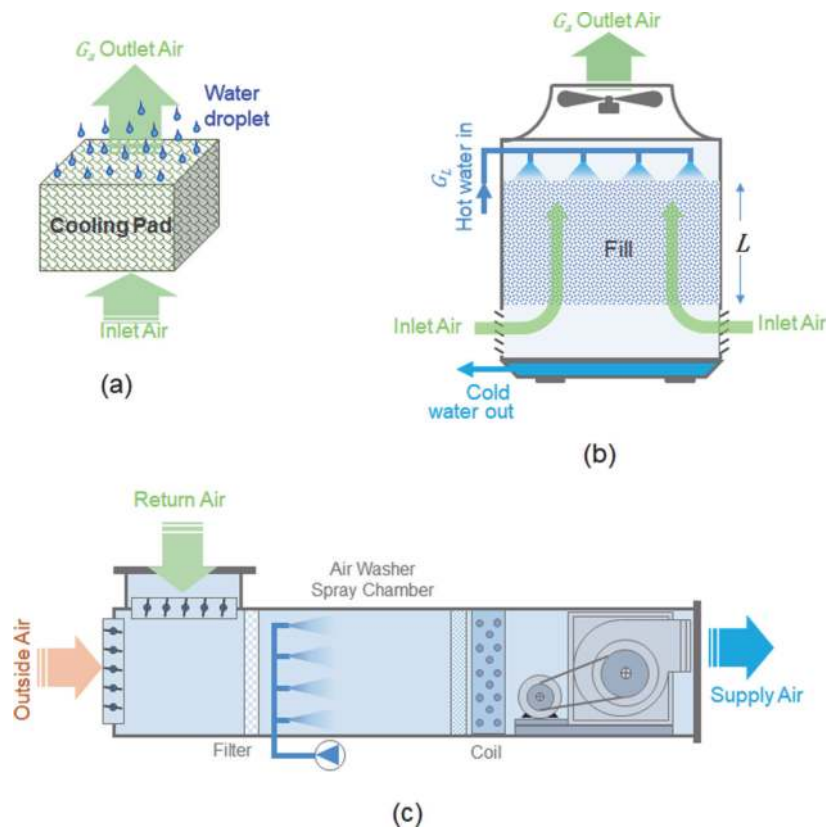


Figure 2. Two fluids direct contact (TFDC) heat exchanger: (a) direct evaporative cooler/swamp cooler, (b) cooling tower, and (c) air washer chamber.

that is wetted with water by dripping or spraying. The air becomes cool and humidified (process 2) after passing through the medium that results from the absorption of heat from the air by the evaporation of water droplets or water film of the cool pad. For it is a passive cooling device, it has a very efficient electrical energy consumption, and so that, it is a very efficient space cooling in the hot and dry region with the lowest initial cost and operation cost.

(2) Cooling tower, shown in **Figure 2(b)**, is not an air conditioner device, but it is used extensively as a heat sink or heat removal from the condenser of the refrigeration circuit in the air conditioning industry. Likewise, in a swamp cooler, the hot water, carrying the rejection heat from the condenser, can be cool down by evaporating its water droplet or water film from the fill. In the cooling tower, the hot water is cooling down as the air stream is heated up and humidified (process 2) by transferring heat and mass between these two fluids.

(3) Air washer spray chamber, shown in **Figure 2(c)**, is a typical DCHME, which is widely used as an air conditioner and works in synergy with the heating or cooling coil in the air handling unit (AHU). The air washer chamber has the capability to condition the inlet air into three desired outlet air state-points by controlling the spraying water temperature. Heating and humidification, like process 4, can be achieved by spraying hot water into the chamber if its spray temperature is higher than the inlet air dry-bulb temperature. Cooling and dehumidification, like process 8, can be achieved by spraying chilled water which temperature is lower than the dew point temperature of the inlet air of the chamber. The inlet air can also be cooled as per process 2 line without changing the moisture content of air by spraying the chilled water temperature, which is lower than the inlet air dry-bulb temperature but higher than its dew point temperature.

Different structures but similar to another type of DCHME are plate finned tube heat exchanger used as a direct expansion (DX) evaporator coil, cooling coil operating with chilled water, or non-volatile refrigerant, shown in **Figure 3(a)**. Indirect evaporative cooler, shown in **Figure 3(b)**, and M-cycle dew point evaporative cooler, shown in **Figure 3(c)**, is also another type of DCHME. These types of exchangers have three fluid streams in which two streams directly contact each other, and the last stream is separated by the copper tube wall or separator sheet, shown in **Figure 3**.

(4) Plate finned tube heat exchangers are the most common type of heat exchanger used extensively in the air conditioning industry using as a DX evaporator coil and cooling coil operating with chilled water or ethylene/propylene glycol. For this case, if the dew point temperature of inlet air is lower than the surface temperature of the exchanger, the air stream's water vapor starts turning into condensate as a form of droplets or film on its surface. Therefore, depending on the dew point and surface temperature, the exchanger, can be thoroughly wetted, fully dry, or partially wetted. The fully dry or dry part of a partially wetted exchanger cannot be presumed as a heat and mass exchanger but as a conventional heat exchanger that can be calculated by its traditional LMDT or NTU-effectiveness

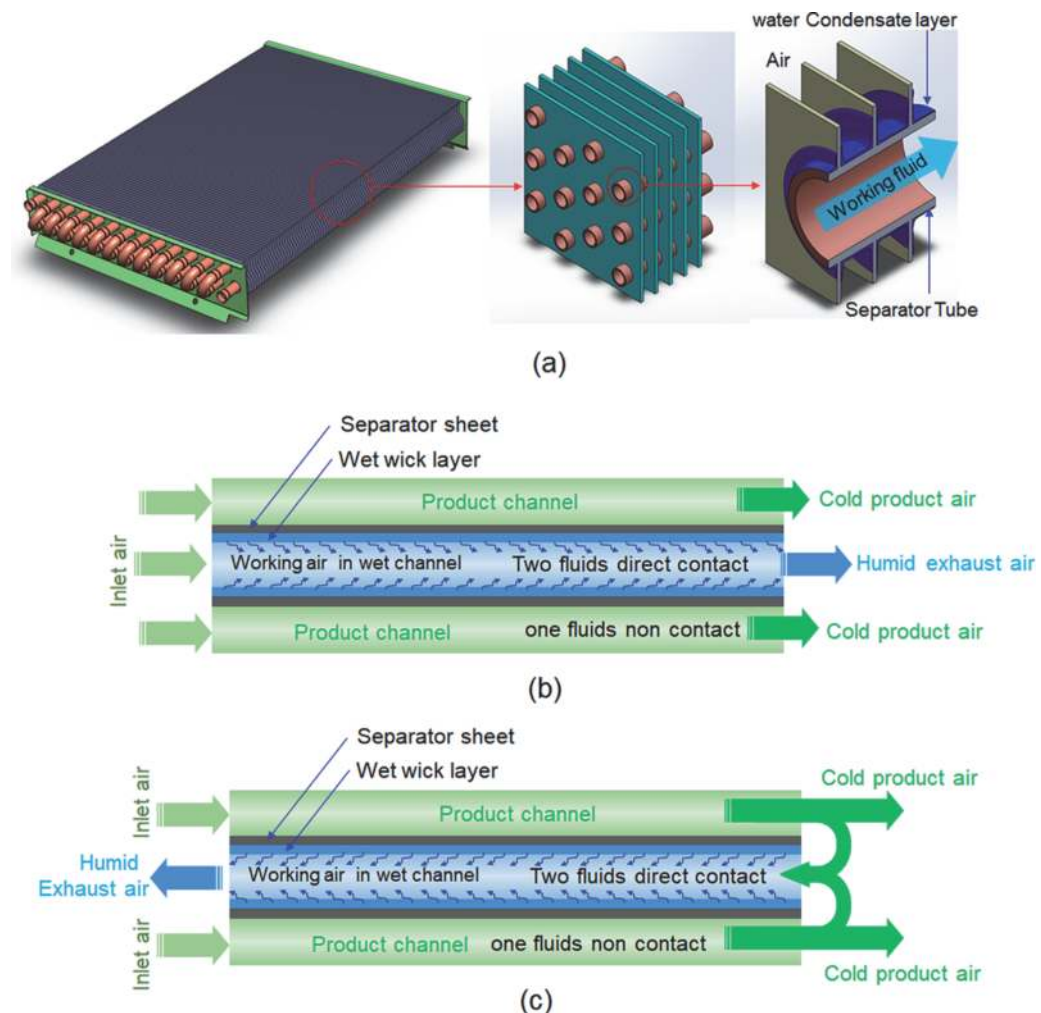


Figure 3. Two direct contact with one non-contact fluids (TDCONF) heat and mass exchanger: (a) plate finned-tube heat exchanger operating with non-volatile or volatile working fluid, (b) indirect evaporative cooler, (c) M-cycle dew point evaporative cooler.

method. However, the fully wetted or wet part of the partially wetted exchanger is a direct contact heat and mass exchanger because heat and mass are exchanged between the two fluids of the air stream and the film of water condensate [2], shown in **Figure 3(a)**. The process rendering in the wet region of this exchanger is cooling and dehumidification of the air stream as process 8.

(5) Indirect evaporative cooler and M-cycle dew point evaporative cooler, shown in **Figure 3(b)** and **(c)**, are a combination of a direct evaporative cooler and air to the air heat exchanger. These coolers are composed of multiple duo wet and dry channels separated by a thin film sheet. The working air flowing through the wet channel is directly in contact with a thin water film of wick material or water mist sprayed into the wet channel for the evaporation process. The required heat for the evaporation is transferred from the product air flowing in the dry channel through the separator sheet. Thus, the product air temperature is cooling down along process 1 without changing the moisture content. For the indirect evaporative cooler, the working air at the beginning of the wet channel will be cooled and humidified like process 2 due to evaporation, but later part of the wet channel, the product air is heated and humidified due to the heat that transfers from the product air, like process 4. Likewise, indirect evaporative cooler, M-cycle dew point evaporative cooler has a similar process, but there has a concise process 2 at the beginning of the wet channel because the working air is partially taken from the product air [3–5].

Based on the number of fluids flowing in the exchanger and their arrangement, DCHME for air conditioning can be categorized into two main groups, which are shown in **Figure 4**. In the first group, the two fluids streams, water, and air are flowing in parallel or counter flow direction and directly contacting each other to exchange heat and mass between these two fluids. This type of exchanger is noted as Type-1 two fluids direct contact (TFDC) heat and mass exchanger. Examples of these exchangers are: (1) air washer chamber, (2) cooling tower, and (3) swamp cooler or direct contact evaporative cooler, shown in **Figure 2**. A single discretized element of this type of TFDC exchanger is shown in **Figure 5**.

The second group of DCHME has three kinds of working fluids in which two fluids, water, and air, are directly contacting each other to exchange heat and mass between these two fluids. The third fluid is separated by a tube wall or a thin sheet

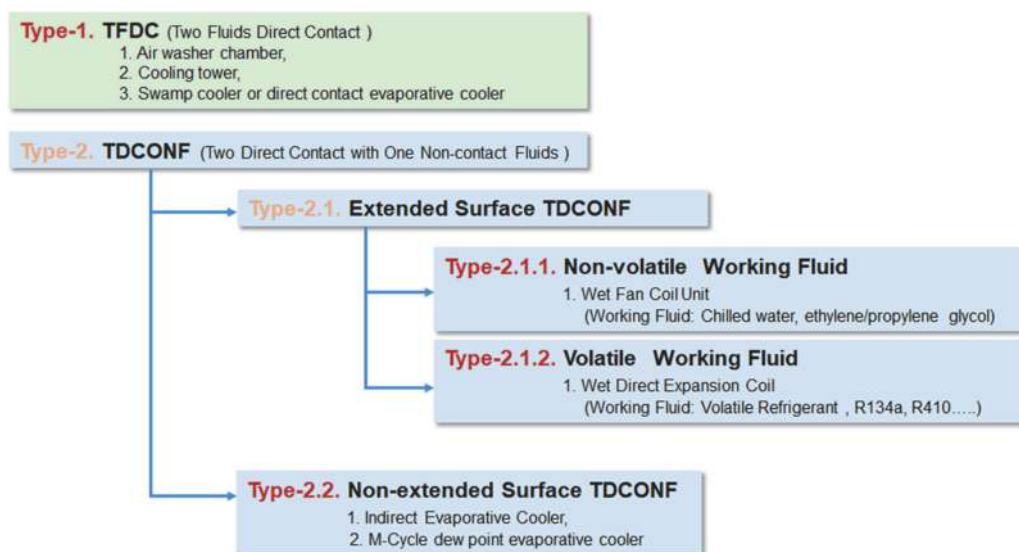


Figure 4. Categorization of direct contact heat and mass exchangers that widely used in air-conditioning industry.

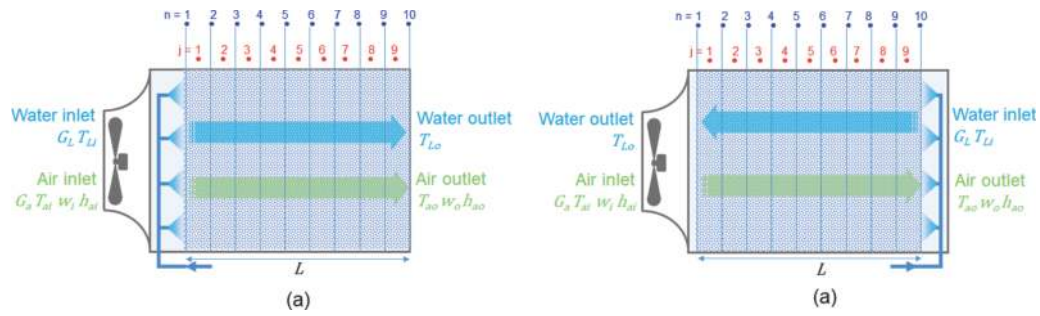


Figure 5.

TFDC exchanger with nine discretized elements, $j = 9$ and $n = 10$, and water is spraying into a (a) parallel or (b) counter flow with air flow direction.

layer to prevent mass transfer but only allow heat transfer. Examples of this type of heat and mass exchanger are shown in **Figure 3**, and it can be noted as Type-2, two direct contacts with one non-contact fluid (TDCONF) heat and mass exchanger. This TDCONF exchanger can also be divided into two groups based on the separator type. The first group, Type-2.1 has a separator with an extended surface. An example of an extended surface TDCONF exchanger is the wet region of the plate finned-tube cooling coil unit. Based on the nature of the working fluid, Type-2.1 can be sub-categorized into two groups. The first group, Type-2.1.1 of extended surface TDCONF exchanger, works with non-volatile refrigerants such as chilled water, ethylene/propylene glycol, etc., so that the working fluid temperature is changing continuously along with the coil rows depth. The second group, Type-2.1.2, works with volatile refrigerants such as R134a, R410, etc. Due to the evaporation in the working fluid flow, most of the exchanger has the same surface and fluid temperature profile. Although these two subgroups are the same exchanger, their mathematical models are different due to their different working fluid temperature profiles. Another group, Type-2.2 non-extended surface TDCONF exchangers, are using a plain sheet or tube as a separator, and examples of this type of exchangers are in the direct evaporative cooler and M-cycle dew point evaporative cooler. The mathematical model of this exchanger is the same with Type-2.1.1 of extended surface TDCONF exchanger except for the separator's area calculation.

Kays and London [6] introduced the definitions of effectiveness and NTU method to use in heat exchanger design in their 1955 publication. London et al. [7] used this method to fit the experimental data of the cooling tower, but this method is not generally consistent with all the other units [8]. The reason for the inconsistency is that the method was based only on the sensible heat transfer process, yet the mass exchanging process is excluded. Berman [9] introduced the log-mean enthalpy method (LMED) to reflect both the heat and mass transfer process of cooling tower design. Several studies used this method to analyze heat and mass exchangers, such as cooling towers and spray chambers [9–11]. LMED method can calculate the dependent parameters and effectiveness of the exchanger without using iteration process, but this method has some limitations to calculate all the parameters of the spatially distributed system. Thus, discretized volume with distributed lumped-parameters method is an alternative approach to develop the exchanger model with element nodes. This method is widely used to study the behavior of spatially distributed parameters of electrical systems [12], chemical reaction systems [13], heat and mass transfer [14, 15], microwave [16, 17], acoustics [18], and so many other systems. In this study, discretized volume with distributed lumped-parameters model was developed for both types of exchangers, Type-1 TFDC and Type-2 TDCONF, based on the principle of the graphical method mentioned in ASHRAE Fundamentals Handbook [19] and Systems and Equipment

Handbook [20]. The derivation of the model for Type-1 TFDC is explained in Section 3, and for Type-2 TDCONF exchanger is described in Section 4. The relation of convective heat transfer with mass transfer coefficients between air and water film, which are related to both models, is explained in Section 2.

2. The relation between convective heat and mass transfer coefficient

All types of DCHME mentioned above can be assumed that each exchanger has similar geometry and boundary conditions for heat and mass transfer process so convective mass transfer is analogous to convective heat transfer, and that can be applied for both laminar and turbulent flows [19]. Bird et al. [21] and Incropera and DeWitt [22] defined the analogy Nusselt (Nu) and Sherwood (Sh) number for the calculation of mass transfer coefficient h_M [m/s] from the heat transfer coefficient α_a [W/m².K]. Nusselt (Nu) number, related with α_a , is a function of Reynold (Re) and Pantanal (Pr) number, expressed in Eq. (1). Sherwood (Sh) number, related with h_M , is a function of Reynold (Re) and Schmidt (Sc) number, stated in Eq. (2).

$$Nu = \frac{\alpha_a D_H}{k_a} = a [Re]^b [Pr]^{1/3} \quad (1)$$

$$Sh = \frac{h_M D_H}{D_v} = a [Re]^b [Sc]^{1/3} \quad (2)$$

where a and b are coefficient numbers, D_H [m] is characteristic length of exchanger, k_a [W/m.K] is thermal conductivity of air, and D_v [m²/s] is mass diffusivity. Division of Eq. (1) with Eq. (2) are called the Reynold analogy, and it gives the relation of Lewis (Le) number which can be seen in Eqs. (5) and (6).

$$\frac{\alpha_a}{h_M} = \left[\frac{Pr}{Sc} \right]^{1/3} \frac{k_a}{D_v} \quad (3)$$

$$\frac{\alpha_a}{h_M} = \left[\frac{Pr}{Sc} \right]^{1/3} \frac{C_p \mu}{Pr} \frac{\rho Sc}{\mu} = Le^{-1/3} Le \rho C_{p_m} \quad (4)$$

$$\frac{\alpha_a}{h_M \rho C_{p_m}} = Le^{2/3} \approx 1 \quad (5)$$

where μ [N s/m²] is dynamic viscosity, C_{p_m} [J/kg.K] is specific heat capacity of moist air, and ρ [kg/m³] is density of air. For the humidity ratio is taken as a driving force in mass transfer process, mass transfer coefficient should be defined with the term $K_M = h_M \rho$ [kg/m².s]. The Lewis relation equation Eq. (5) can be written as follows:

$$\frac{\alpha_a}{K_M C_{p_m}} = Le^{2/3} \approx 1 \quad (6)$$

Similarly, Chilton and Colburn [23] proposed Chilton-Colburn j-factor analogy using this similarity to relate Nusselt number to friction factor by the analogy. The j-factor analogy has some limitation that is it can be only reliable when the surface conditions are identical. Bedingfield and Drew [24] also proposed the relation equation between heat and mass coefficients. Many others relation equations that can be found in literatures to calculate mass transfer coefficient h_M from heat transfer coefficient α_a , but in this study, Lewis relation will use in this model development due to its simplicity.

3. Type-1: two fluids direct contact (TFDC) exchanger

TFDC heat exchangers, such as air washer chamber, cooling tower, and swamp cooler or direct contact evaporative cooler, are the first type of DCHME shown in **Figure 2**. TFDC has two water and air fluids flowing in parallel or counter, and directly contacting each other to exchange heat and mass between them. **Figure 6(a)** shows the basic one discretized element of air washer spray chamber and direct contact evaporative cooler. The air stream is directly in contact with the saturated layer of each water droplet or the fill/cool pad, and heat and mass are transferring between them according to the mass transfer coefficient K_M with mass transfer area a_M and heat transfer coefficient α_a with heat transfer area a_H . **Figure 6(b)** shows the fundamental discretized element of the cooling tower and swamp cooler. Both elements have the same concept of numbering node for three layers parameters; air and its average, water and its average, and saturated layer parameters, shown in **Figure 6(c)**.

3.1 Energy balance between two fluids of Type-1 model (energy balance line, EBL)

In TFDC exchanger, the water is sprayed into the chamber along the airflow (parallel flow), shown in **Figure 5(a)**, or against the airflow (counter flow), shown in **Figure 5(b)**. Due to the difficulty of area measurement, TFDC exchangers are discretized in length along the fluids flowing, assuming it has same cross sectional area. **Figure 5** shows that the system is divided into nine differential volumes numbered by “ j ,” and the inlet and outlet of the differential volumes are noted by “ n .” Since each differential volumes has the same cross sectional area, the differential volume can be changed with differential length “ dL .” and mass flowrates of water and air are needed to be changed to mass flux or flow rate per unit cross-sectional area of the exchanger, A_{CS} [m^2], for air G_a [$kg/(s \cdot m^2)$], and water G_L [$kg/(s \cdot m^2)$].

According to the conservation of energy, the energy transferred from one fluid is equal to the energy gain of the other fluid. Assuming that heat loss from the

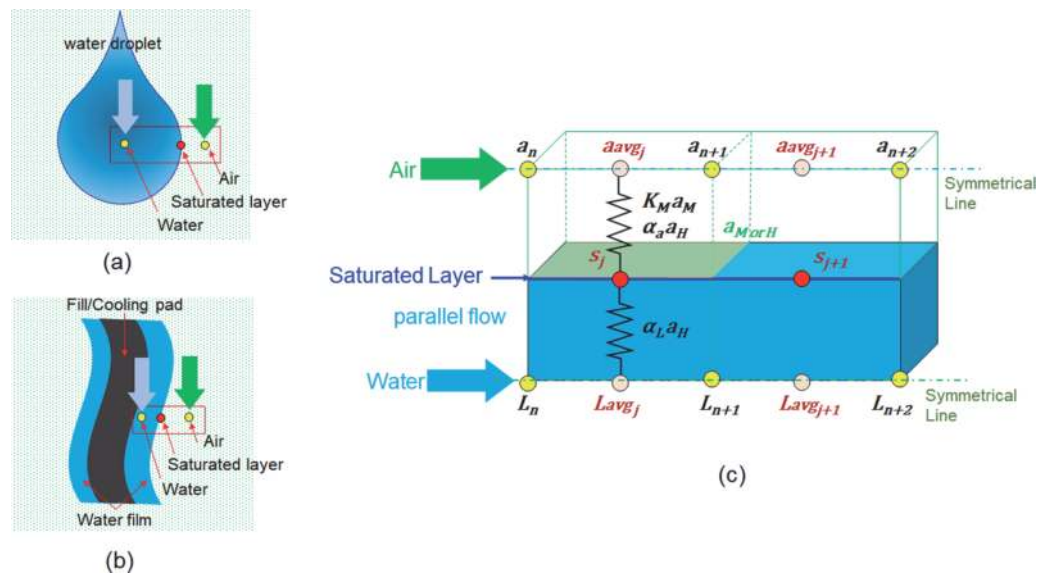


Figure 6. (a) Single discretized element of the air washer spray chamber or direct contact evaporative cooler, and (b) of cooling tower or swamp cooler, and (c) node numbering of the points for air stream, water flow, and saturated layer of each element.

system and the change of air or water flow rate due to evaporation or condensation are comparatively small and negligible. Hence, the energy equation of two fluids can be expressed as follows:

$$G_a dh_a = -G_l C_{p_l} dT_l \quad (7)$$

where, dh_a [kJ/kg] and dT_l [°C] are the enthalpy and temperature difference between outlet and inlet of one discretized element, and Eq. (7) can be rewritten with element node number for the parallel and counter flow as follows:

$$\frac{h_a^{n+1} - h_a^n}{T_l^{n+1} - T_l^n} = -\frac{G_l C_{p_l}}{G_a} \quad (8)$$

$$\frac{h_a^{n+1} - h_a^n}{T_l^n - T_l^{n+1}} = -\frac{G_l C_{p_l}}{G_a} \quad (9)$$

The generalized energy balance line equation with node number for the counter and parallel flow can be described as follows:

$$\frac{h_a^{n+1} - h_a^n}{T_l^{n+1} - T_l^n} = \pm \frac{G_l C_{p_l}}{G_a} \quad (10)$$

A minus sign refers to parallel flow of air and water stream. A plus sign refers to counter flow (water flow is in the opposite direction of airflow).

3.2 Heat and mass transfer between two fluids of Type-1 model (tie-line slope, TLS)

According to the conservation of mass between the two fluids, change of water amount in liquid stream, dG_l , due to evaporation (if saturated humidity ratio, w_s [kg/kg], at the saturated layer is greater than humidity ratio, w_a , of air stream) or condensation (if $w_s < w_a$) is equal to the amount of humidification or dehumidification of air stream, $-G_a dw_a$, in the spray chamber. The above statement can be expressed by equation as follows:

$$\Delta mass = dG_l = -G_a dw_a \quad (11)$$

The negative sign means that the increasing of mass in one fluid stream is equal to the losing mass of other fluid stream. Similarly, the change of mass flow rate, $\Delta mass$ from either stream is equal to the mass flux [kg/m²], that is, mass transfer from the air stream to the saturated liquid surface (or) vice versa per contact surface area along the exchanger, A_{CT} [m²]. It can be written in equation as follows:

$$\Delta mass = K_M a_M (w_s - w_{avg}) dL \quad (12)$$

where, K_M [kg/(s·m²)] is mass transfer coefficient, that is, mass transfer rate per contact surface area along the exchanger, A_{CT} [m²]. a_M [m²/m³] is a mass transferring contact surface area between air and water per unit volume of spray chamber. L [m] is the chamber length. The sensible heat transfer between air stream and saturated liquid surface can be expressed as follows:

$$G_a C_{p_m} dT_a = \alpha_a a_H (T_s - T_{avg}) dL \quad (13)$$

where, α_a [$W/(m^2 \cdot K)$] is convective heat transfer coefficient of air. a_H [m^2/m^3] is heat transfer contact surface area between air and water per unit volume of spray chamber. C_{pm} [$kJ/(kgda \cdot K)$] is a specific heat of moist air at constant pressure. T_s [$^{\circ}C$] is saturation temperature of water film. T_{avg} [$^{\circ}C$] is the average air temperature of two adjacent nodes, see in **Figure 6(c)**. The total heat transfer between air stream and saturated liquid surface is equal to the sum of sensible heat, $C_{pm}dT_a$, and latent heat, $h_{fg}dw$. The total heat transfer can be calculated by combining of mass transfer Eq. (12) multiplying with enthalpy of vaporization h_{fg} [kJ/kg] and the sensible heat transfer Eq. (13). The total heat transfer equation can be expressed as follows:

$$G_a(C_{pm}dT_a + h_{fg}dw) = [K_M a_M (w_s - w_{avg})h_{fg} + \alpha_a a_H (T_s - T_{avg})]dL \quad (14)$$

Since $C_{pm}dT_a + h_{fg}dw$ is equal with enthalpy change of air dh_a , and a small change of water vaporization heat with the function of temperature is neglected, the Eq. (14) can be rewritten as follows:

$$G_a dh_a = K_M a_M \left[(w_s - w_{avg})h_{fg} + \frac{\alpha_a a_H}{K_M a_M} (T_s - T_{avg}) \right] dL \quad (15)$$

The contact surface areas per system volume, a_H and a_M for the heat and mass transferring process in spray chambers are identical ($a_H = a_M$), however, this hypothetical is not always correct, especially, if the systems are using the packing materials as an extension of contact surface area which are not fully wetted. Assuming Lewis number with the power of 2/3 is similar with 1, see in Eq. (6), and neglecting of a small variations in h_{fg} . McElgin and Wiley [25] simplified Eq. (15) as follows:

$$G_a dh_a = K_M a_M (h_s - h_{avg})dL \quad (16)$$

The sensible heat transferring from saturated liquid surface to the working fluid stream is equal to the heat gain of the working fluid, the energy balance equations can be depicted as follows:

$$G_l C_{pl} dT_l = \alpha_l a_H (T_s - T_{lavg})dL \quad (17)$$

After substitution of Eqs. (16) and (17) into Eq. (7), and rearranged, the Eq. (7) can be written as follows:

$$-\alpha_l a_H (T_s - T_{lavg})dL = K_M a_M (h_s - h_{avg})dL \quad (18)$$

$$\frac{h_s - h_{avg}}{T_s - T_{lavg}} = -\frac{\alpha_l a_H}{K_M a_M} = -\frac{\alpha_l C_{pl}}{\alpha_a} \quad (19)$$

According to the above Eq. (19), the value of, $-\frac{\alpha_l C_{pl}}{\alpha_a}$, is a slope or gradient line of the rise, the enthalpy incensement in vertical over the run, temperature incensement along the horizontal in T-h graph. In other words, the slope is a ratio of the enthalpy difference between air and saturated surface to the temperature difference between working fluid and saturated surface. This slope, the relation of the temperature and enthalpy, can be denoted as tie-line slope, *TLS* of the Type-1 TFDC exchanger. The *TLS*, Eq. (19), can be solved by using graphical method, drawing in water-air T-h graph which is proposed in [2, 19, 20, 26], but this method cannot be applied in the numerical model. In order to solve *TLS* equation numerically, the two unknown parameters, saturated temperature, T_s , and saturated enthalpy, h_s , have to

reduce one unknown parameter by substitution of their relation equation that can be obtained by fitting of the saturation line on T-h graph, calculated from the psychrometric chart equations depicted in ASHRAE code [19], with the third order polynomial regression equation, Eq. (20).

$$h_s = coe1.T_s^3 + coe2.T_s^2 + coe3.T_s + coe4 \quad (20)$$

Figure 7 shows the third order polynomial regression line with the saturation point, in red circle legend, calculated by psychrometric chart equations, and its four related coefficients values, *coe1* to *coe4*. The regression has a very high accuracy as its R-square value 0.9993706, which covering the range of air temperature from 0 to 50°C.

By the substitution of polynomial regression equation Eq. (20) into Eq. (19), the tie-line slope equation become one unknown parameter equation, and that can be rewritten with node number *n* and *j* as follows:

$$coe1(T_s^j)^3 + coe2(T_s^j)^2 + (coe3 + TLS)T_s^j + coe4 - \left(\frac{h_a^n + h_a^{n+1}}{2} \right) - TLS \left(\frac{T_l^n + T_l^{n+1}}{2} \right) = 0 \quad (21)$$

Newton Raphson iteration method or any other relevant numerical method can be applied to solve out the unknown root value T_s of each node *j* of the equation, Eq. (21), by using the known value of T_l and h_a of each node *n* (node numbering of each element is shown in Figure 6).

3.3 Dry bulb temperature of each node for Type-1 model

The last unknown parameter of air temperature, T_a [°C], of each node *n*, can be calculated from the ratio of sensible heat Eq. (13) to total heat and mass transfer Eq. (16), and it gives as follows:

$$\frac{dT_a}{dh_a} = \frac{\alpha_a a_H (T_s - T_{avg})}{K_M C_{pm} a_M (h_s - h_{avg})} \quad (22)$$

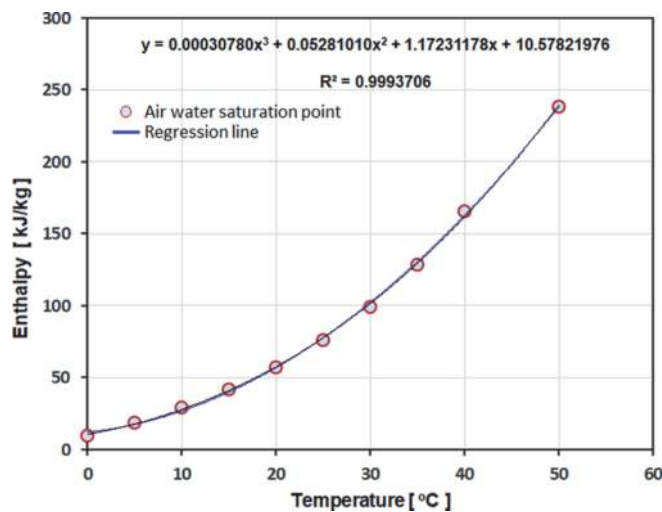


Figure 7.
 Third order polynomial regression equation of the enthalpy of the saturated air.

The value of $\frac{\alpha_a}{K_M C_{pm}}$ can be taken as 1 because the Lewis number with the power of 2/3 is approximately equal to 1, see in Eq. (6). For the TFDC exchanger, this study assumes that the contact surface area per volume of heat transferring process, a_H , is identical with the one of mass transferring process, a_M . For numerical calculation, the average parameters, T_{aavg} and h_{aavg} , are located between two adjacent n nodes, and noted with j node, shown in **Figure 6**. After rearranging of the Eq. (22), it gives with node number n and j as follows:

$$T_a^{m+1} - T_a^m = \frac{\frac{h_a^{n+1} - h_a^n}{(h_s^j - h_{aavg}^j)} (T_s^j - T_a^m)}{\left(1 + \frac{h_a^{n+1} - h_a^n}{2(h_s^j - h_{aavg}^j)}\right)} \quad (23)$$

The outlet air temperature of each node, T_a^{m+1} , can be calculated from the known inlet temperature, T_a^m , air enthalpy, h_a , average air enthalpy, h_{aavg} , vapor saturated air enthalpy, h_s , and vapor saturated air temperature, T_s by using Eq. (23).

3.4 Contact length calculation for Type-1 TFDEC exchanger model

Calculation of the contact length or depth of packing of the exchanger, L [m], is a primary interest for the designing of the system to achieve a desired out let condition of air or out let water temperature. The length can be calculated by the integration of heat and mass transfer equation, Eq. (16).

$$L = \frac{G_a}{K_M a_M} \int_{j=1}^{j=N-1} \frac{1}{(h_s - h_{aavg})} dh_a \quad (24)$$

The integral equation, Eq. (24) can be solved by using Sampson's rule or Trapezoidal integration method. The integral equation can be rearranged and rewritten with node number n and j as follows:

$$L = \frac{G_a}{K_M a_M} \sum_{j=1}^{j=N-1} \left[\frac{1}{(h_s^j - h_{aavg}^j)} \times (h_a^{n+1} - h_a^n) \right] \quad (25)$$

Change of the air mass flow rate, G_a , due to the transfer of water vapor from the water droplet or film to the air by evaporation or condensation is very minimal compared with its mass flowrate, and it can be taken as negligible for all the practical applications. The contact length or exchanger length L , can be calculated from the known air enthalpy, h_a , and saturated enthalpy, h_s , of each elements.

4. Type-2: two direct contact with one non-contact fluids (TDCONF) exchanger

Section 1, discussed about the DCHME that widely used in air conditioning industry, has categorized the exchangers into two groups. Mathematical model of the first type TFDC heat exchanger has been discussed in Section 3. The development of mathematical model for the second type of TDCONF exchanger will be discussed in detail in this section. The examples of TDCONF exchangers are the wet region of plate finned tube heat exchanger for the direct expansion (DX) evaporator coil, cooling coil unit working with chilled water or non-volatile refrigerant,

indirect evaporative cooler, and M-cycle dew point evaporative cooler, which are shown in **Figure 3**.

A discretized volume with distributed lump parameters model of TDCONF, shown in **Figure 8**, has three fluids, non-contact fluid, contact fluid, and wetted wick layer or thin water film. The product air of indirect evaporative cooler and volatile refrigerant or chilled water of the wetted plate finned tube cooling coil are the examples of non-contact fluid. These fluids are separated by the separator sheet or tube from thin water film and contact fluid air to prevent the transferring of mass and only to allow the transferring of heat between non-contact fluid and thin water film. Thermal resistance due to the conduction of separator sheet or metal tube is R_{mw} , and due to the convective heat transfer in the non-contact fluid is R_l . But, both heat and mass are transferring between the thin water film and contact fluid air. Heat and mass transfer circuit between from the symmetrical line of contact fluid air to the non-contact fluid with the coefficient of mass transfer, K_M , and thermal resistances are shown in **Figure 8(c)**. Each discretized volume of all TDCONF exchanger is composed with three node points locating in line on the four layers of materials. The first node point, L_{avgj} is at the symmetrical line of non-contact fluid, s_j is at the surface of saturated water film, and a_{avgj} is at the symmetrical line of direct contact fluid air. This model assumed that the temperature difference between outer surface of separator sheet or copper tube and saturated surface of water film is negligible. TDCONF exchanger can be divided into three types of different numerical models: (1) Type-2.1.1 extended surface TDCONF exchanger working with non-volatile working fluid, (2) Type-2.1.2 extended surface TDCONF exchanger working with volatile refrigerant, and (3) Type-2.2 non-extended surface TDCONF exchangers, shown in **Figure 4**.

4.1 Type-2.1: Extended surface TDCONF exchanger

In air conditioning process, plate finned tube heat exchange are widely used for cooling and dehumidification process in fan coil unit (FCU) and air handling unit (AHU). If there is no condensation on the outer surface of finned tube heat exchanger, it is a normal heat exchanger and can be calculated by using conventional heat exchanger equation, UA-LMTD or NTU-effectiveness method.

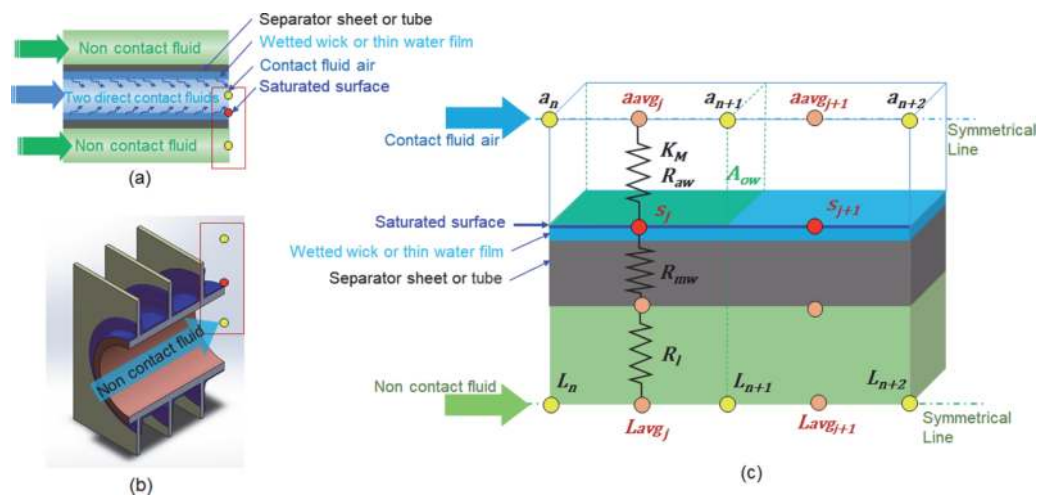


Figure 8. A discretized volume with distributed lump parameters model of a typical (a) indirect evaporative cooler, (b) wetted region of plate finned tube cooling coil, and (c) node numbering of non-contact fluid (product air, volatile refrigerant, and chilled water), water saturated surface layer, separator (sheet or tube), and contact fluid (air).

However, if the surface temperature of heat exchanger is lower than the dew point temperature of the direct contact fluid air, the condensation process will be taken place and not only heat but also mass will be transferred between the air flow and the water condensate film. Hence, wet region of cooling heat exchanger can be assumed as a direct contact heat and mass exchanger.

4.2 Fin efficiency of extended surface TDCONF heat exchanger

In plate finned tube heat exchanger, fin efficiency is one of the critical parameters for the development of exchanger model, and that can be calculated from the physical dimensions of the heat exchanger. Equations (26)–(33) are the equations to calculate the physical parameters of heat exchanger; number of fins N_f [–], coil face or frontal area A_a [m²], external exposed prime surface area A_p [m²], external secondary surface area A_s [m²], internal surface area A_i [m²], total external surface area A_o [m²], the ratio of external to internal surface area Br [–], and coil core surface parameters F_s [–] from its dimensions, width L_W [m], height L_H [m], depth L_D [m], fin gap f_g [m], fin thickness f_t [m], outside d_o [m], inside diameter d_i [m] of tube, longitudinal tube spacing S_L [m], and transverse tube spacing S_T [m]. This equations are based on heat exchanger with the continuous plate fin and tubes in stagger arrangement. For the other type of heat exchanger, their related equations are stated comprehensively in AHRI standard 410 [27], and that can be applied in the fin efficiency calculation.

$$N_f = \frac{L_W}{f_g} \quad (26)$$

$$A_a = \frac{L_H L_W}{1000000} \quad (27)$$

$$A_s = N_f \left[\frac{L_H L_D}{500000} - \frac{d_o^2 N_t}{636688} \right] \quad (28)$$

$$A_p = \frac{d_o L_W N_t - d_o f_t N_t N_f}{318344} \quad (29)$$

$$A_i = \frac{d_i N_t L_W}{318344} \quad (30)$$

$$A_o = A_s + A_p \quad (31)$$

$$Br = \frac{A_i}{A_o} \quad (32)$$

$$F_s = \frac{A_o}{A_f N_r} \quad (33)$$

Fins can increase heat transfer from a prime surface of heat exchanger. Fin efficiency can be define with the ratio of the actual heat transferred from the fin to the heat that would be transferred if the entire fin were at its root or base temperature [20]. Fin efficiency equation can be written as follows:

$$\varnothing_f = \frac{\int \alpha_a (T_f - T_a) dA}{\int \alpha_a (T_{fr} - T_a) dA} \quad (34)$$

where \varnothing_f is the fin efficiency, T_a is the temperature of the surrounding environment, and T_{fr} is the temperature at the fin root. T_f is the temperature along the

fin. Fin efficiency decreases as the heat transfer coefficient increases because of the increased heat flow. Total heat transfer from a finned tube heat exchanger is sum of heat transfer from finned surface or secondary area A_s and un-finned or prime area A_p . It can write in equation as follows:

$$Q = (\alpha_p A_p + \phi_f \alpha_s A_s) (T_{fr} - T_a) \quad (35)$$

Assuming the heat transfer coefficients for the finned surface α_s and prime surface α_p are equal and note as α_a air side heat transfer coefficient, Eq. (35) can be rearranged as follows:

$$\phi_s = \left(1 - (1 - \phi_f) \frac{A_s}{A_o} \right) = \frac{A_p + \phi_f A_s}{A_o} \quad (36)$$

where A_o is total surface area of $(A_s + A_p)$. ϕ_s is fin effectiveness. Schmidt [28] presents empirical equation of fin surface efficiency for circular, rectangular, and hexagonal fins using an equivalent circular fin radius.

$$\phi_f = \frac{\tanh(m_p r_o \phi)}{m_p r_o \phi} \quad (37)$$

$$m_p = \sqrt{\frac{2 \alpha_a}{k_a t_f}} \quad (38)$$

$$\phi = \left[\left(\frac{r_e}{r_o} \right) - 1 \right] \left[1 + 0.35 \ln \left(\frac{r_e}{r_o} \right) \right] \quad (39)$$

where r_o is the outside tube radius, r_e is the equivalent circular fin radius, m_p is the standard extended surface parameter, ϕ is dimensionless thermal resistance. α_a is convective heat transfer coefficient of air. k_a is the thermal conductivity of the fin and t_{fin} is the fin thickness. Plate finned tube heat exchanger for stagger tube array can be considered as the integration of hexagonal fins. For hexagonal fins:

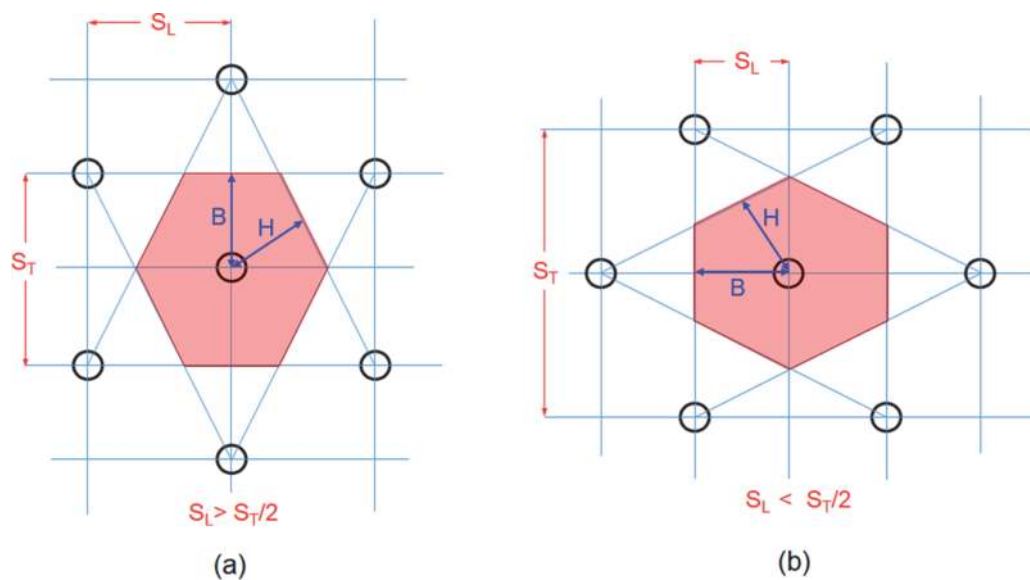


Figure 9. Staggering arrangement of tube in plate finned tube heat exchanger (a) a half of transverse distance is lesser than longitudinal distance and (b) longitudinal distance is lesser than half of transverse distance.

$$\frac{r_e}{r_o} = 1.27 \psi \sqrt{\beta - 0.3} \quad (40)$$

where Ψ and β are defined as; $\psi = B/r_o$ and $\beta = H/B$, β must be greater than 1. Depending on the ST (the transverse vertical tube spacing) and SL (the longitudinal horizontal tube spacing), shown in **Figure 9**, B and H can be defined as follows:

If $SL > ST/2$, then $B = ST/2$. If $SL < ST/2$, then $B = SL$.

$$H = \frac{1}{2} \sqrt{\left(\frac{ST}{2}\right)^2 + SL^2} \quad (41)$$

However, Schmidt's empirical equation of fin surface efficiency is limited to the situations of where $\beta > 1$.

When calculating the overall area of Type-2.1 extended surface TDCONF exchanger, the fin effectiveness term, ϕ_s , can be used to simplify the thermal resistance equation of heat and mass transfer from air to working fluid.

4.3 Type-2.1.1 extended surface TDCONF exchanger operating with non-volatile working fluid

Type-2.1.1 extended surface TDCONF exchanger is widely used as a cooling coil of air conditioning unit that operating with non-volatile working fluid such as chilled water or ethylene/propylene glycol. The air entering to the first part of the cooling coil is start decreasing its temperature but without moisture removing, this is called sensible heat removing part or dry coil region. When the air temperature is decreasing and reaching the dew point temperature of the entering air, moisture in the air stream start condensing on the surface of the coil called sensible and latent heat removing part or wet coil region.

4.3.1 Resistance of heat and mass transfer and dry-wet boundary region

Depending upon the dew point temperature of inlet air and working fluid temperature, the surface of the cooling coil can be fully dry, fully wet, or partially wet. The driving force for heat transfer in dry region is the temperature difference between air temperature T_a and working fluid temperature T_l , crossing the thermal resistance R_{ad} , R_{md} , and R_l . In the wet region, there are two types of heat and mass transfer processes synergy in series from the air to the working fluid. The first process is the exchange of heat and mass between the air and the saturated surface of water condensate layer due to their potential difference between h_a and h_s . The second process is transferring heat alone from the surface to the working fluid, and their driving force is the temperature difference between T_s and T_l . **Figure 10** shows a typical plate finned tube heat exchanger with counter flow process and thermal diagram of dry and wet region with their potential difference and resistances.

The capacity of the sensible heat Q_D that transferring in the dry region can be calculated by using the following equation:

$$Q_{Td} = U_D A_{oD} \Delta T_m = \frac{A_{oD} \Delta T_m}{R_{TD}} \quad (42)$$

where A_{oD} [m^2] is total surface area of dry region, R_{TD} [$m^2.K/W$] is total thermal resistance of dry region, and ΔT_m is log mean temperature difference between air dry bulb temperature and working fluid temperature. In wet region, total heat

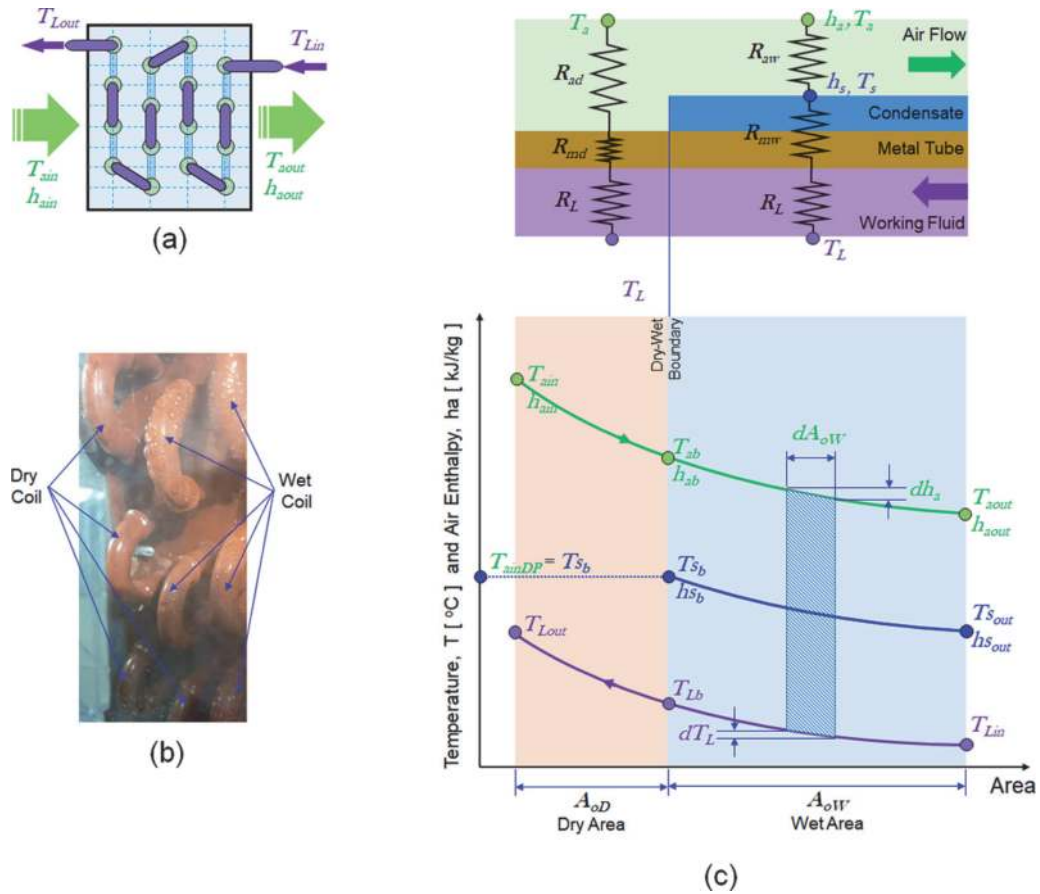


Figure 10. (a) A typical single circuit with four rows deep coil plate finned tube heat exchanger with counter flow arrangement between air and working fluid, (b) photo record of dry and wet region, and (c) thermal diagram of dry and wet region of extended surface TDCONF exchanger and their potential difference of heat and mass transfer process.

capacity, Q_W , sensible heat and latent heat, transferred from air to saturated surface of condensate water can be calculated by using the following equation:

$$Q_{Tw} = U_W A_{oW} \Delta h_m = \frac{A_{oW} \Delta h_m}{Cp_m R_{aW}} \quad (43)$$

where A_{oW} [m^2] is total surface area of wet region, R_{aW} [$\text{m}^2 \cdot \text{K/W}$] is thermal resistance of air side in wet region, and Δh_m is log mean enthalpy difference between air and saturated wetted surface layer. For the calculation of heat transfer from air to working fluid, total overall thermal resistance of finned tube heat exchanger is required to calculate from the heat exchanger parameters and heat transfer coefficient. Overall thermal resistance with clean non-fouled surfaces for dry and wet cooling coils is a combination of three individual thermal resistances: (1) R_a [$\text{m}^2 \cdot \text{K/W}$] convective thermal resistance between air and external surface of the coil, (2) R_m [$\text{m}^2 \cdot \text{K/W}$] total conductance heat transfer of the metal fin, R_f , and tube, R_t , and (3) R_l [$\text{m}^2 \cdot \text{K/W}$] convective thermal resistance between the internal surface of the coil and the working fluid flowing inside the coil. Brown [29] derived thermal resistance of dry region, R_{md} , and wet region, R_{mw} , based on the heat transfer concept, proposed by Ware-Hacha [30], as follows:

$$R_{md} = R_f + R_t = \frac{(1 - \phi_s)}{\phi_s} R_{ad} + \frac{Br D_i \ln(D_o/D_i)}{2 k_t} \quad (44)$$

$$R_{mw} = R_f + R_t = \frac{(1 - \phi_s)}{\phi_s} \left(R_{aw} \frac{Cp_m}{m} \right) + \frac{Br D_i \ln(D_o/D_i)}{2 k_t}. \quad (45)$$

where m'' is $\frac{dh_s}{dT_s}$. The overall thermal resistance of dry R_{Td} and wet R_{Tw} region can be calculated as follows:

$$R_{Td} = R_{ad} + R_{md} + R_l = \frac{1}{\phi_s \alpha_{ad}} + \frac{Br D_i \ln(D_o/D_i)}{2 k_t} + \frac{Br}{\alpha_l}. \quad (46)$$

$$R_{Tw} = R_{aw} + R_{mw} + R_l = \frac{1}{\alpha_{aw}} + \frac{(1 - \phi_s)}{\phi_s} \left(\frac{1}{\alpha_{aw}} \frac{Cp_m}{m} \right) + \frac{Br D_i \ln(D_o/D_i)}{2 k_t} + \frac{Br}{\alpha_l}. \quad (47)$$

where R_{ad} , R_{aw} [$m^2.K/W$] are thermal resistance for convective heat transfer between air and external surface of the dry and wet coil, R_t [$m^2.K/W$] is thermal resistance of the metal tube, and R_l [$m^2.K/W$] is thermal resistance between the internal surface of tube and the working fluid flowing inside the coil. Br [-] is the ratio of total external surface area A_o to internal surface area A_i .

The ratio of wet and dry coil region is influenced by the characteristic of coil such as coil arrangement, refrigerant distribution, coil depth, entering air dew point and dry bulb temperatures, working fluid temperature, and their flowrates. Another parameter, Y [$kg \text{ } ^\circ C/kJ$], the ratio of fluid temperature rise to air enthalpy drop, is also important parameter to calculate the boundary region. Y can be driven from the ratio of the heat that gained by working fluid to the heat that lost from the air stream. The equation is as follows:

$$\frac{dT_l}{dh_a} = \frac{m_a}{m_l Cp_l} = Y \quad (48)$$

The total heat transferring from the air to the saturated water surface in wet region of TDCONF exchanger is similar with TFDC exchanger, Eq. (16). Mass transfer coefficient K_M is substituted with Eq. (6), and it can be written as follows:

$$dq_{Tw} = K_M (h_a - h_s) dA_{ow} = \frac{(h_a - h_s) dA_{ow}}{Cp_m R_{aw}} \quad (49)$$

Total heat transferred capacity dq_{Tw} in wet region also equals with the heat that transfer from the saturated wet surface layer to the working fluid that flowing inside the tube.

$$dq_{Tw} = \frac{(T_s - T_l) dA_{ow}}{R_{mw} + R_l} \quad (50)$$

After equating and rearranging of Eqs. (49) and (50), the following equation will be obtained, and can be denoted as the characteristic of the coil, C [2, 19, 20, 26].

$$C = \frac{R_{mw} + R_l}{Cp_m R_{aw}} = \frac{(T_s - T_l)}{(h_a - h_s)} \quad (51)$$

For the dry-wet boundary line, the coil characteristic C can be expressed as follows:

$$C = \frac{(T_{dpai} - T_{lb})}{(h_{ab} - h_{sb})} \quad (52)$$

Enthalpy of air at dry-wet boundary line, h_{ab} [kJ/kg] can be derived from Eqs. (48) and (52) as follows:

$$h_{ab} = \frac{T_{dpai} - T_{lo} + Y h_{ai} + C h_{sb}}{C + Y} \quad (53)$$

The exchanger coil can be determined whether it is fully wetted, fully dry, or partially wetted by comparing the values of h_{ab} with h_{ai} , and h_{ao} . If the value h_{ab} is higher than h_{ai} , all the surface of exchanger is fully wetted. If the value of h_{ab} is higher than h_{ao} but less than h_{ai} , the surface of exchanger is partially wetted. If the value of h_{ab} is less than h_{ao} , then the surface of exchanger is completely dry. The temperature of air at dry-wet boundary point, T_{ab} [°C], can be calculated from the heat energy equation of the air stream that flowing in dry region.

$$T_{ab} = T_{ai} - \frac{(h_{ai} - h_{ab})}{Cp_m} \quad (54)$$

The working fluid temperature at dry-wet boundary line, T_{lb} [°C], can be calculated from the energy balance equations between the air stream and working fluid in the dry region.

$$T_{lb} = T_{lo} - Y Cp_m (T_{ai} - T_{ab}) \quad (55)$$

Air temperature, air enthalpy, and working fluid temperature of dry region can be calculated by using traditional heat exchanger equations. But for the wet region, a discretized volume with distributed lump parameters method, like TFDC model that explained detail in Section 3, can calculate the parameters of air stream, saturated surface, and working fluid.

4.3.2 Energy balance between two fluids of Type-2.1.1 exchanger (energy balance line, EBL)

Energy balance line for the wet region of Type-2.1.1 exchanger can be derived by equating the energy lost from the air stream and the energy gained by the working fluid. EBL equation for each element with the numbering, n , of each node can be expressed as follows:

$$m_a dh_a = -m_l Cp_l dT_l \quad (56)$$

$$\frac{h_a^{n+1} - h_a^n}{T_l^{n+1} - T_l^n} = \pm \frac{m_l Cp_l}{m_a} = EBL \quad (57)$$

A minus sign refers to a parallel flow between air stream and working fluid flow. A plus sign refers to a counter flow that working fluid is flowing in the opposite direction of airflow.

4.3.3 Heat and mass transfer between two fluids of Type-2.1.1 model (tie-line slope)

Tie-line slope is the ratio of enthalpy difference between air and saturated surface to the temperature difference between working fluid and saturated surface. Tie-line slope, Eq. (59) can be derived from the equating of the sensible heat, transferring from the working fluid to saturated surface, with the total sensible and latent heat that transferring from the saturated surface to the air stream, see in

Figure 10. Tie-line slope of Type-2.1.1 extended surface TDCONF exchanger is similar with the one of TFDC exchanger, Eq. (19), but the difference is an addition of thermal resistances of the metal wall and fins in the wet region, R_{mw} . Hence, Tie-line slope for Type-2.1.1 extended surface TDCONF exchanger can be expressed with the characteristic of coil, C , as follows:

$$K_M(h_s - h_{aavg})dA = U_{sl}(T_{lavg} - T_s)dA \quad (58)$$

$$\frac{h_s - h_{aavg}}{T_s - T_{lavg}} = -\frac{U_{sl}}{K_M} = -\frac{Cp_m R_{aw}}{R_{mw} + R_l} = -\frac{1}{C} = -TLS \quad (59)$$

The total heat which is transferring from the saturated surface node j , T_s^j to the average temperature of air stream, T_{lavg}^j which is the average of two adjacent nodes temperature T_l^n and similarly from the saturated surface to the air stream are shown in **Figure 11**. TLS equation, Eq. (59), has two unknown parameters, saturated temperature, T_s , and saturated enthalpy, h_s . The third order polynomial regression equation, which is fitted with the saturation 100% RH line, shown in **Figure 7**, can be used as their relation equation Eq. (20) to the TLS equation Eq. (59), and rearranged with node number as follows:

$$coe1(T_s^j)^3 + coe2(T_s^j)^2 + (coe3 + TLS)T_s^j + coe4 - \left(\frac{h_a^n + h_a^{n+1}}{2}\right) - TLS\left(\frac{T_l^n + T_l^{n+1}}{2}\right) = 0 \quad (60)$$

This third order polynomial TLS equation can be solved by using Newton Raphson iteration methods to finds its unknown root parameter, T_s , from the known parameters of tie line slope, enthalpy of air, and working fluid temperature.

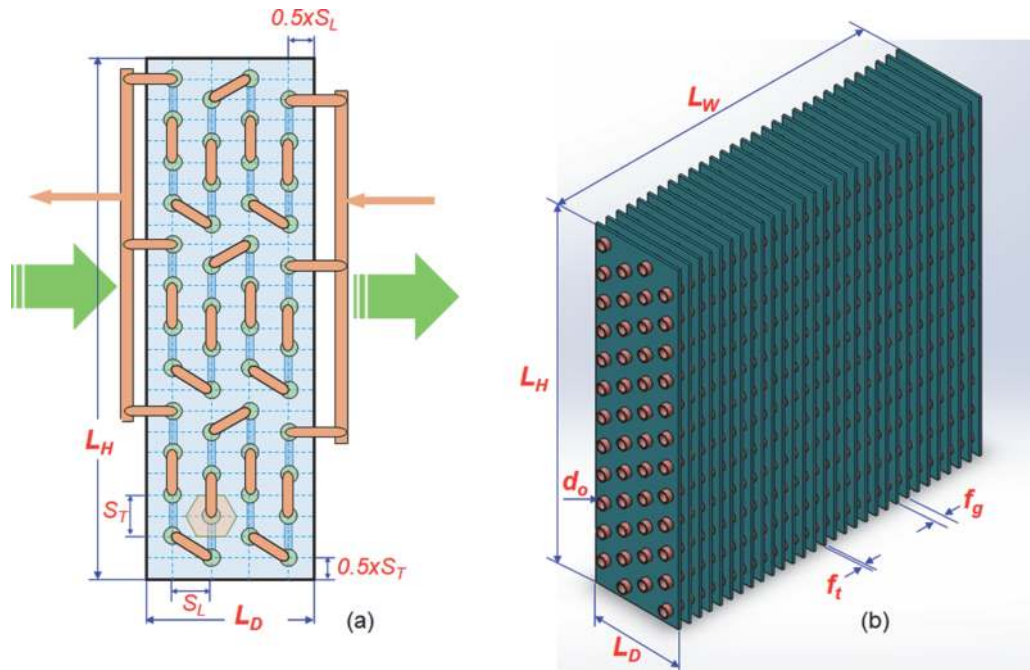


Figure 11. Typical plate finned tube heat exchange with (a) a three circuit tube with four rows deep and staggered arrangement and, (b) its 3D view with dimensions' notation.

4.3.4 Dry bulb temperature of each node for Type-2.1.1 model

Likewise the derivation of air temperature in Section 3.3, the air temperature of each node of TDCONF exchanger can be driven from the ratio of sensible heat that transfer from air to saturated surface to the total heat and mass transfer from the air to saturated surface. The ratio is as follows:

$$\frac{m_a C_{pm} dT_a}{m_a dh_a} = \frac{\alpha_{aw} (T_s - T_{aavg}) dA}{K_M (h_s - h_{aavg}) dA} \quad (61)$$

The value of $\frac{\alpha_{aw}}{K_M C_{pm}}$ can be assumed 1 for the Lewis number to the power of 2/3 is similar with 1, see the derivation in Section 3.2. For numerical calculation, the air temperature of each node, Eq. (61) is needed to be rearranged and rewritten with node number n and j as follows:

$$T_a^{n+1} - T_a^n = \frac{\frac{h_a^{n+1} - h_a^n}{(h_s^j - h_{aavg}^j)} (T_s^j - T_a^n)}{\left(1 + \frac{h_a^{n+1} - h_a^n}{2(h_s^j - h_{aavg}^j)}\right)} \quad (62)$$

From the above equation outlet air temperature of each node T_a^{n+1} can be calculated from the known parameters of air inlet temperature, air enthalpy, and saturated air enthalpy of each node.

4.3.5 Exchanger area calculation of Type-2.1.1

The area of wet region, A_w , can be calculated by integration of the energy balance equation which is the total heat losing from the air stream is equal to the total heat and mass transferring from the air stream to the vapor saturated surface layer.

$$\int m_a dh_a = \int K_M (h_s - h_{aavg}) dA \quad (63)$$

Mass transfer coefficient, K_M , can be substituted with the parameters $\frac{\alpha_{aw}}{C_{pm}}$, as the Lewis number to the power of 2/3 is similar with 1, see in Eq. (6). The integral equation Eq. (63) can be solved out with Sampson's rule or Trapezoidal method, and it can rewrite with node number n and j as follows:

$$A_{ow} = \frac{m_a C_{pm}}{\alpha_{aw}} \sum_{j=1}^{j=N-1} \left[\frac{1}{(h_s^j - h_{aavg}^j)} \times (h_a^{n+1} - h_a^n) \right] \quad (64)$$

The wet surface area of TDCONF exchanger can be calculated from the known parameters, air enthalpy h_a and vapor saturated enthalpy h_s of each element.

4.4 Type-2.1.2 extended surface TDCONF exchanger operating with volatile working fluid

The exchanger's geometrical structure of Type-2.1.2 is the same with the one of Type-2.1.1, for both are using plate finned tube heat exchanger having a similar thermal resistance for heat and mass transferring from air to working fluid. But the

difference between them is that Type-2.1.1 exchanger is working with non-volatile fluid so that its fluid temperature T_L is increasing along the area axis from T_{Lin} to T_{Lout} , shown in **Figure 10**, and Type-2.1.2 exchanger is operating with volatile refrigerant so that its working fluid temperature is constant along the coil depth, dT_L is 0. As a result, the parameter Y become infinity. For coil characteristic C for Type-2.1.2 is similar with Type-2.1.1, the margin point, h_{ab} , of dry and wet region of Type-2.1.2 exchanger can be calculated from the coil characteristic equation Eq. (65). At boundary point, water saturated surface temperature of dry and wet region is same as dew point temperature of inlet air, $T_s = T_{dpai}$. The enthalpy of air at boundary, h_{ab} can be expressed as follows:

$$h_{ab} = h_{sb} + \frac{(T_{dpai} - T_l)}{C} \quad (65)$$

Similarly with Type-2.1.1, temperature of air at dry-wet boundary point can be calculated from the equation, Eq. (65). As the working fluid temperature is constant in all coil depth, fluid temperature at boundary point T_{Lb} is same as with T_L . Energy balance line for Type-2.1.2 is vertical for its refrigerant temperature is constant along the coil depth, dT_L is 0. As a result, the refrigerant temperature of each node is constant, and the enthalpy of air outlet h_{ao} can be calculated from the energy balance equation between the total heat lost from the air stream and the vaporization heat of the refrigerant, and the equation is as follows:

$$m_a dh_a = -m_l h_{fg}(T_r) \quad (66)$$

$$h_{ao} = h_{ai} - \frac{m_l h_{fg}(T_r)}{m_a} \quad (67)$$

The equations of tie-line slope, dry bulb air temperature, and contact area for Type-2.1.2 are the same with Eqs. (60), (62), and (64).

4.5 Type-2.2: non-extended surface TDCONF heat exchanger

Indirect evaporative cooler and M-cycle dew point evaporative cooler, Type-2.2 exchangers, are passive coolers and very efficient cooler for dry and hot region. The two fluids, a thin water film and working air, are directly contacting each other, and they do not contact with the third fluid, product air, by separating with aluminum or plastic film to prevent the moisture transferring and make sure allowing only heat transfer.

The phenomena of heat and mass transfer and its mathematical model is the same with a wet region of Type-2.1.1 exchanger, except the calculation of separator area. Tube is used as separator in Type-2.1.1 exchanger and flat sheet is used in Type-2.2 exchanger. Thus, total thermal resistance, RT , of non-extended surface TDCONF exchanger can be written with convective heat transfer coefficient of working air, α_{aw} , and of product air, α_{ap} . k_{sep} is the thermal conductivity of the separator and t_{sep} is the separator thickness. The total resistance equation can be expressed as follows:

$$RT = R_{aw} + R_{mw} + R_{ap} = \frac{1}{\alpha_{aw}} + \left(\frac{1}{\alpha_{aw}} \frac{Cp_m}{m} \right) + \frac{t_{sep}}{k_{sep}} + \frac{1}{\alpha_{ap}} \quad (68)$$

The rest equations of energy balance line (EBL), tie-line slope (TLS), dry bulb air temperature T_a , and contact area for Type-2.2 exchanger are the same with Eqs. (57), (60), (62), and (64).

5. Effectiveness of heat and mass exchanger

The effectiveness of heat and mass exchanger are defined in many different ways in many studies. The effectiveness of cooling tower, and direct evaporative cooler based on the temperature is the ratio of the range, the change of water temperature between the inlet, T_{Lin} , and the outlet, T_{Lout} , to the sum of the range and the approach which is the difference between water outlet temperature and the inlet air wet-bulb temperature, T_{WBain} [31], expressed as follows:

$$\varepsilon_{CoolingTower} = \frac{Range}{Range + Approach} = \frac{T_{Lin} - T_{Lout}}{T_{Lin} - T_{WBain}} \quad (69)$$

Although Jaber and Webb [8] proposed a modified definition of cooling tower effectiveness with enthalpy, temperature based effectiveness, Eq. (69), is widely used in the cooling tower industry and this study also. Saturation effectiveness is a key factor in the determination of direct and indirect evaporative cooler performance. The saturation effectiveness of direct evaporative cooler is the ratio of the dry bulb temperature difference between inlet air, T_{DBain} , and outlet air T_{DBaout} , to the difference between inlet air dry bulb temperature and its wet bulb temperature, T_{WBain} [2], expressed as follows:

$$\varepsilon_{DirectEvapCooler} = \frac{T_{DBain} - T_{DBaout}}{T_{DBain} - T_{WBain}} \quad (70)$$

The saturation effectiveness of indirect evaporative cooler, wet-bulb depression efficiency, is the ratio of the dry bulb temperature difference between the product air inlet, T_{DBpain} , and outlet, $T_{DBpaout}$, to the difference between the product air inlet and inlet wet bulb temperature of working air, T_{WBwain} [2], expressed as follows:

$$\varepsilon_{IndirectEvapCooler} = \frac{T_{DBpain} - T_{DBpaout}}{T_{DBpain} - T_{WBwain}} \quad (71)$$

The effectiveness of air washer chamber and wet part of cooling coil are based on the enthalpy, and can be defined as the ratio of enthalpy difference between air inlet and out let to the difference between inlet air enthalpy and saturation enthalpy associated with working fluid inlet temperature [8, 32], expressed as follows:

$$\varepsilon_{Coil/Airwasher} = \frac{h_{ain} - h_{aout}}{h_{ain} - h_{SWFin}} \quad (72)$$

6. Results and discussion

This study has developed four types of numerical models for DCHME widely used in the air-conditioning industry. The first model explained in Section 3 is for Type-1 TFDC exchanger: air washer chamber, cooling tower, swamp cooler, or direct contact evaporative cooler, shown in **Figures 2, 5, and 6**. The second model derived in Section 5.2 is for Type-2.1.1 extended surface TDCONF exchanger working with non-volatile refrigerant (2.1.1. Extended Surface-Non Vol). An example of these exchanges is the wet region of plate finned tube heat exchanger used for cooling and dehumidification working with chilled water or ethylene/propylene glycol, shown in **Figures 3(a), 8(b) and (c), and 10**. The third model derived in Section 5.3 is for Type-2.1.2 extended surface TDCONF exchanger working with

volatile refrigerant (2.1.2. Extended Surface-Vol). Examples of these exchangers are the wet region of DX-coil for cooling and dehumidification working with R134a, R410, etc., shown in **Figures 3(a)** and **8(b)** and **(c)**. Finally, the fourth model, derived detail in Section 6, is for Type-2.2 non-extended surface TDCONF exchanger (2.2. Non-Extended Surface), which are indirect evaporative cooler and M-cycle dew point evaporative cooler, shown in **Figures 3(b)**, **8(a)** and **(c)**, and **12**.

There are two types of problems with known (given) parameters and parameters to calculate for DCHME, which are listed in **Table 1**. The first type of problem, Case 1a, and 1b, is the case for designing DCHME to solve the length or area of the exchanger to achieve the desired fluid outlet temp or air outlet condition. The second type of problem, Case 2, is the case for the model predictive control system to predict the effectiveness and output parameter of a given DCHME under the load's variation and different operational parameters. Model 1. TFDC and 2.1.1. Extended Surface-Non Volatile working fluids have three problem cases, but model 2.1.2. Extended Surface-Vol has only two problems excluded Case 1b because there is no temperature difference between the inlet and outlet of the volatile working fluid. Similarly, model Type-2.2. Non-Extended Surface has no Case 1a because the product air operating as a working fluid is the only parameter needed to design and develop the control model of the exchanger. The models with different types of problem cases are shown in **Figure 13**.

Figure 14 shows the simulation result of temperature and enthalpy of the air, water, and saturated layer of each element of Type-1 TFDC exchanger, which are cooling tower or air washer chamber with Case 1 problem, calculation of exchanger

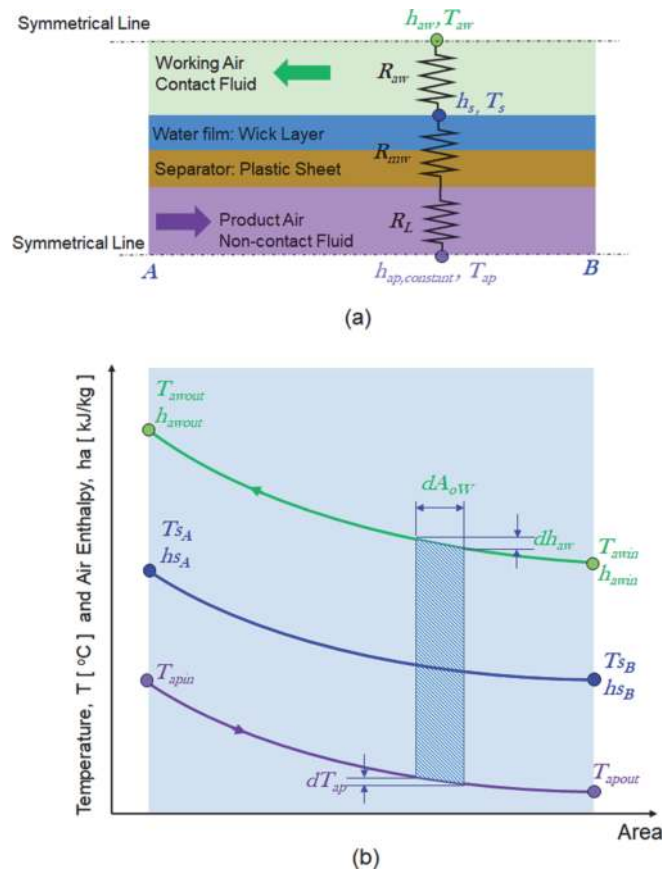


Figure 12.

(a) A typical one unit cell of non-extended TDCONF exchanger with counter flow process between product air and working air, and (b) thermal diagram of non-extended surface TDCONF exchanger and their potential difference for heat and mass transfer process.

Problem types	Known parameters	Parameters to calculate
Case 1a [Parallel/Counter] Calculation of length or area of exchanger to get the desired working fluid outlet temp.	1. Both inlets [$T_{ai}, w_i T_{Li}$] 2. Both flowrates [G_a, G_L] TFDC [m_a, m_L] TDCONF 3. Working fluid outlet [T_{Lo}] 4. Heat transfer coef. [$\alpha_a a_H, \alpha_L a_H$] TFDC [α_a, α_L] TDCONF	1. Air outlet condition [T_{ao}, w_o] 2. Saturate line [T_s, h_s] 3. Length [L] or area [A_w]
Case 1b [Parallel/Counter] Calculation of length or area of exchanger to get the desired air outlet condition.	1. Both inlets [$T_{ai}, w_i T_{Li}$] 2. Both flowrates [G_a, G_L] 3. Air outlet condition [T_{ao}, w_o, h_a] 4. AW heat transfer coef. [$h_{aa}H, h_{La}H$] PFTHEx thermal resistance	1. Working fluid outlet [T_{Lo}] 2. Saturate line [T_s, h_s] 3. Length [L] or area [A_w]
Case 2 [Parallel/Counter] Prediction of the effectiveness and the working fluid outlet temp or air outlet condition of exchanger with known length or area.	1. Both inlets [$T_{ai}, w_i T_{Li}$] 2. Both flowrates [G_a, G_L] 3. Length [L] 4. AW heat transfer coef. [$h_a a_H, h_L a_H$] PFTHEx thermal resistance	1. Both outlets [$T_{ao}, w_o T_{Lo}$] 2. Saturate line [T_s, h_s]

Table 1.
List of problem types with known and calculation parameters for DCHME.

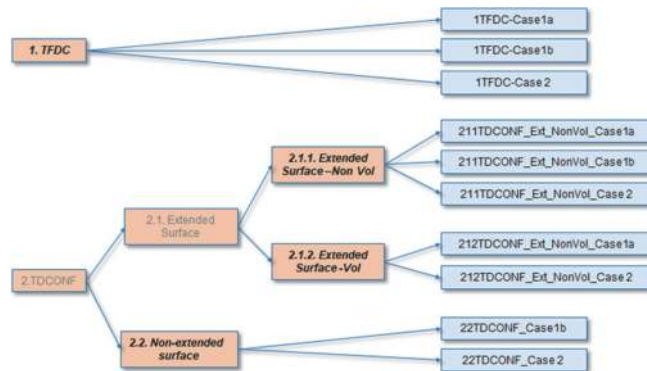


Figure 13.
Four models with three different problem types of air conditioning exchanger.

length or area. The numbering of nodes i and j for exchanger is shown in **Figure 5**, in which water is spraying into an (a) parallel or counter flow with airflow direction. The process is heating and humidifying airflow in the air washer chamber or cooling the water in the cooling tower. **Figure 14(a)** shows the result of parallel flow exchanger where the energy balance line is inclined to the left side due to its negative slope per Eq. (10), and similarly, the positive slope for counter flow, thus the line inclined to the right side as shown in **Figure 14(b)**. Both counter and parallel flow have the same negative tie line slope value, see Eq. (19), both tie lines are inclined into the left side. The outlet air temperature, green circle, of counter flow is 1.5°C higher than parallel flow under all the same condition. Thus, the counter flow has higher efficiency than the parallel flow.

Figure 15 shows the simulation result of temperature and enthalpy of the air, water, and saturated layer of each element of Type-1 TFDC exchanger, air washer

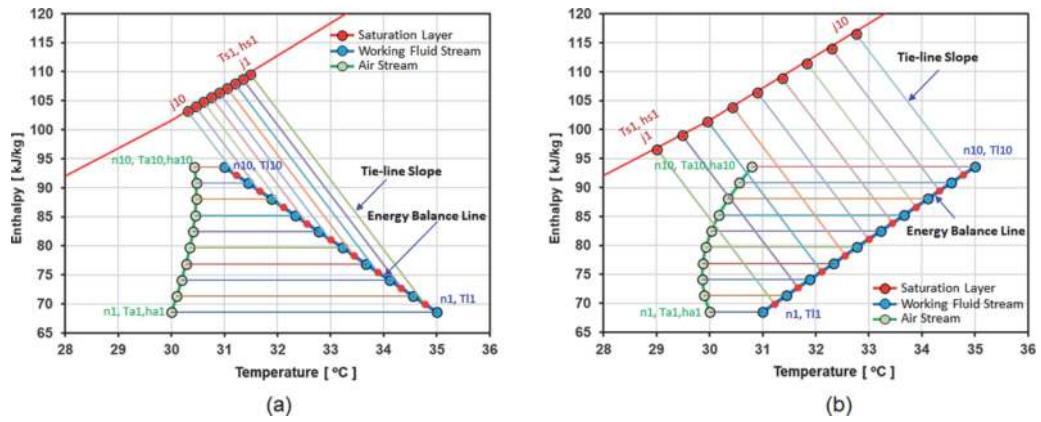


Figure 14. Temperature and enthalpy of air, water and saturated layer of each element of Type-1 TFDC exchanger with Case 1 problem for the process of air heating and humidification in air washer chamber or cooling the water in cooling tower (a) parallel flow, and (b) counter flow.

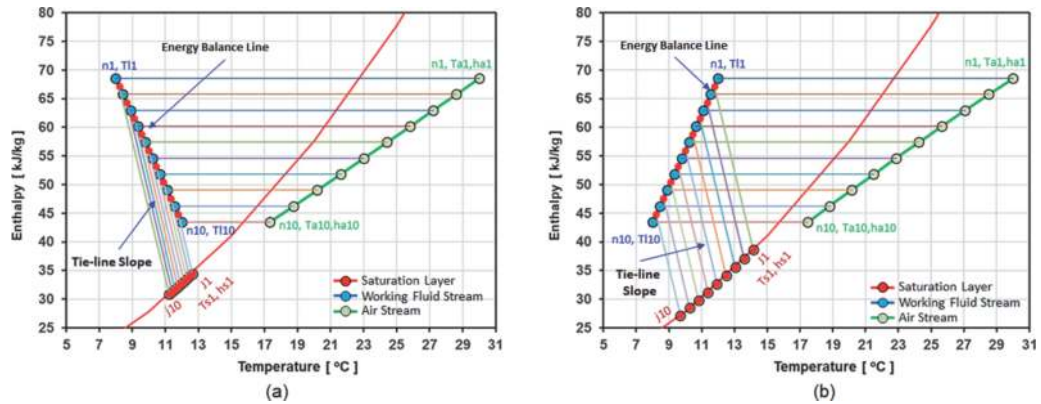


Figure 15. Temperature and enthalpy of air, water and saturated layer of each element of Type-1 TFDC and Type-2.1.1 exchanger with Case 1 problem for the process of air cooling and dehumidification in air washer chamber and cooling coil operating with non-volatile working fluid in a (a) parallel flow, and (b) counter flow.

chamber, Type-2.1.1 exchanger, wet region of cooling coil working with non-volatile fluid, for the process of air cooling and dehumidification. The behavior of the energy balance line and tie line is the same as the heating and humidification process, but the waterline, blue circle, is left side of the saturation line because the working fluid temperature is lower than the saturation temperature, red circle, at each node. At the same time, the water line is on the right side of the saturation line because the working fluid temperature is higher than the saturation temperature in the air heating and humidification process, see **Figure 14**.

Figure 16 shows the effectiveness of the exchanger based on the water stream, Eq. (69), and based on the airflow stream Eq. (72) for cooling tower and air washer chamber under the same giving length with different liquid air ratio and inlet air enthalpy. At a low liquid-air flow ratio, the effectiveness of cooling tower based on water temperature stream is higher because the range, the temperature difference between water inlet and outlet, is higher due to the low water flow rate. However, for the air washer based on air stream, the effectiveness, Eq. (72), is lower than the higher liquid-air flow ratio because the temperature difference between the air inlet and outlet temperature is higher due to the high airflow rate. Therefore, this Type-1 exchanger with the Case 2 problem model can predict the effectiveness and outlet condition of water or air stream under the several of liquid-air flow ratio and inlet

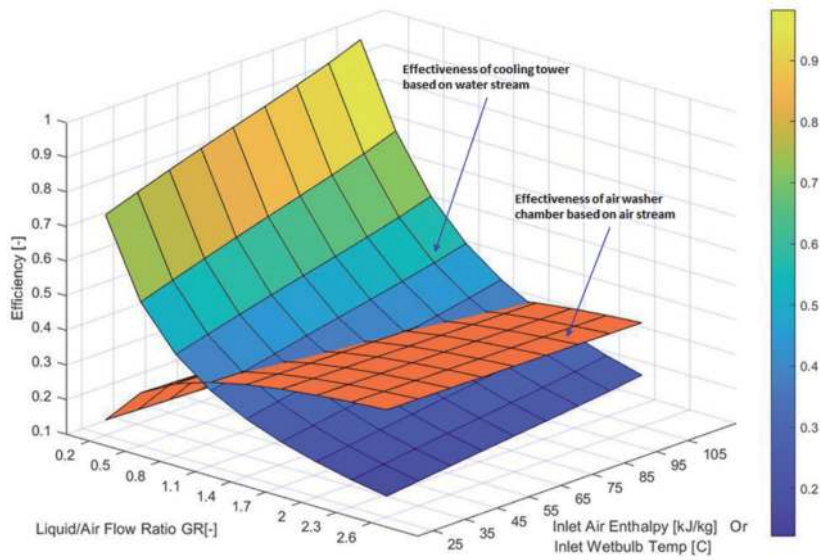


Figure 16. Effectiveness of Type-1. TFDC exchanger based on the water stream for cooling tower and based on the air stream for air washer chamber: Type-1 exchanger with Case 2 problem model.

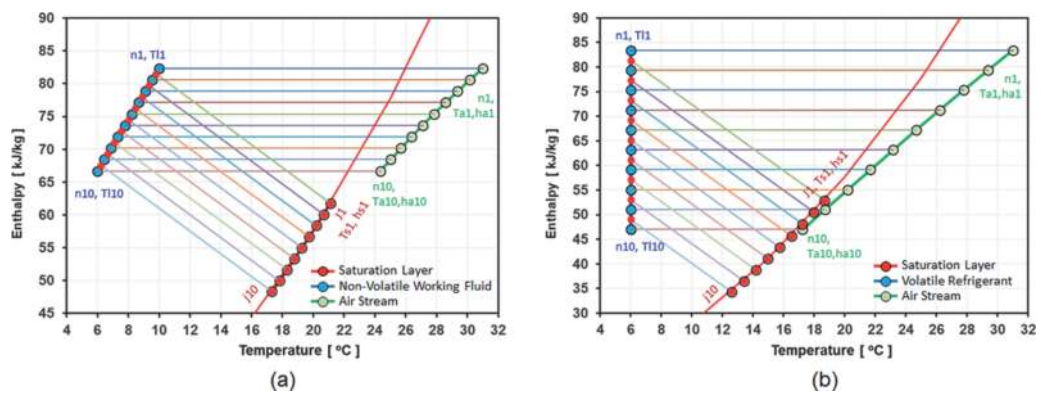


Figure 17. Temperature and enthalpy of each element's (a) air, non-volatile working fluid and saturated layer of Type-2.1.1 exchanger (b) air, volatile working fluid and saturated layer of Type-2.1.2 exchanger with counter flow for the process of cooling and dehumidification.

air condition. Thus this model can be applied as a sub-function of the model predictive control system.

Figure 17 shows the simulation result of the temperature and enthalpy of each element. **Figure 17(a)** depicts the result of the model, Type-2.1.1 extended surface working with the non-volatile working fluid, and **Figure 17(b)** shows the result of the model, Type-2.1.2 extended surface working with volatile refrigerant for the process of cooling and dehumidification. Both models run at 6°C of working fluid temperature with the exact dimension of the plane finned tube heat exchanger and the same flow rate, flow rate ratio, and condition of the inlet air. Depending on the nature of the volatilization of the working fluid, the temperature of the non-volatile working fluid changes from inlet 6°C to outlet 10°C. The outlet air temperature is dropped from 31 to 24.1°C, as shown in **Figure 17(a)**, whereas, in the model of Type-2.1.2, the refrigerant temperature is constant at 6°C, but the outlet air temperature is dropped from 31 to 17°C, as shown in **Figure 17(b)**. Thus, the Type-2.1.2 exchanger has a better performance than the Type-2.1.1 exchanger.

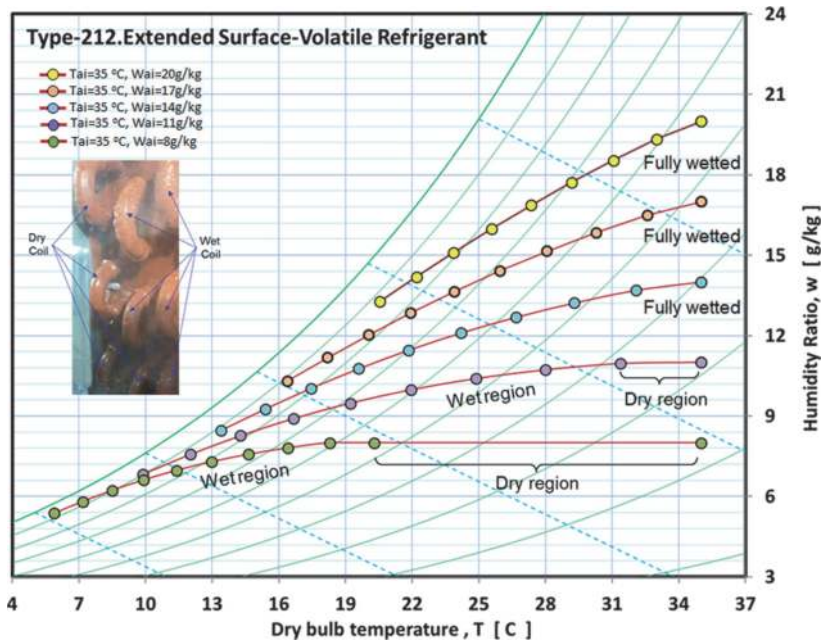


Figure 18. Cooling and dehumidification process of Type-2.1.1 exchanger with same inlet air temperature but different humidity ratio.

Figure 18 shows the simulation result of model Type-2.1.1 exchanger running with the same plate finned tube heat exchanger and operating with the same volatile refrigerant at 5°C with the same refrigerant-air flow ratio. The result clearly shows that the model can estimate the dry and wet area and predict the outlet air temperature and moisture removing rate under different air inlet conditions (same inlet temperature but different humidity ratio). Thus, these models are suitable for use as a sub-function of the model predictive control system.

7. Conclusion

This study has developed a mathematical model based on a discretized volume with distributed lumped-parameters method for two fluid direct contact (TFDC) exchangers and two direct contacts with one non-contact fluid (TDCONF) exchanger. Based on the flow system and structure, this study has developed four models; Type-1 TFDC exchanger model (air washer chamber, cooling tower, and swamp cooler or direct contact evaporative cooler), Type-2.1.1 extended surface TDCONF exchanger model working with non-volatile refrigerant (wet region of plate finned tube heat exchanger cooling coil working with chilled water or ethylene/propylene glycol), Type-2.1.2 extended surface TDCONF exchanger working with volatile refrigerant (wet region of plate finned tube DX-coil), and Type-2.2 non-extended surface TDCONF exchanger (indirect evaporative cooler and M-cycle dew point evaporative cooler). From the simulation result, these models can reflect both heat and mass transfer behavior in every spatially distributed physical system. Moreover, they can predict well the effectiveness and dependent parameters of DCHME under the different load conditions and its various input parameters. Hence, these models can be a valuable tool for designing the exchangers mentioned above and can be applied as a sub-function of the model predictive control system.

Author details

Marip Kum Ja^{1*}, Qian Chen¹, Muhammad Burhan¹, Doskhan Ybyraiymkul¹,
Muhammad Wakil Shahzad², Raid Alrowais³ and Kim Choon Ng¹


1 Water Desalination and Reuse Center, King Abdullah University of Science and
Technology, Thuwal, Saudi Arabia

2 Northumbria University, Newcastle Upon Tyne, United Kingdom

3 Civil Engineering Department, Al Jouf University, Skaka, Saudi Arabia

*Address all correspondence to: mkum.ja@kaust.edu.sa

IntechOpen

© 2022 The Author(s). Licensee IntechOpen. This chapter is distributed under the terms of the Creative Commons Attribution License (<http://creativecommons.org/licenses/by/3.0>), which permits unrestricted use, distribution, and reproduction in any medium, provided the original work is properly cited. 

References

- [1] Jacobs HR. Direct contact heat exchangers. DOI:10.1615/AtoZ.d.direct_contact_heat_exchangers
- [2] 2020 ASHRAE Handbook—HVAC Systems and Equipment (SI). Atlanta, GA: ASHRAE; 2020
- [3] Lin J, Wang RZ, Kumja M, Bui TD, Chua KJ. Modelling and experimental investigation of the cross-flow dew point evaporative cooler with and without dehumidification. *Applied Thermal Engineering*. 2017;**121**:1-13
- [4] Lin J, Thu K, Bui TD, Wang RZ, Ng KC, Kumja M, et al. Unsteady-state analysis of a counter-flow dew point evaporative cooling system. *Energy*. 2016;**113**:172-185
- [5] Lin J, Wang RZ, Kumja M, Bui TD, Chua KJ. Multivariate scaling and dimensional analysis of the counter-flow dew point evaporative cooler. *Energy Conversion and Management*. 2017;**150**:172-187
- [6] Kays WM, London AL. *Compact Heat Exchangers*. New York: McGraw-Hill Companies; 1964
- [7] London AL, Mason WF, Boelter LMK. Performance characteristics of a mechanically induced draft, counter flow, packed cooling tower. *Transactions of ASME*. 1940;**62**:41-50
- [8] Jaber H and Webb BL. Design of cooling towers by the effectiveness-NTU method. *Journal of Heat Transfer*. November 1989;**111**(4):837-843
- [9] Berman LD. Chapter 2. In: Sawistowski H, editor. *Evaporative Cooling of Circulating Water*. 2nd ed. New York: Pergamon Press; 1961. pp. 94-99. [translated from Russian by R. Hardbottle]
- [10] Webb RL. A critical review of cooling tower design methods. In: Shah RK, Subbarao EC, Mashelkar RA, editors. *Heat Transfer Equipment Design*. Washington, DC: Hemisphere Pub. Corp.; 1988. pp. 547-558
- [11] Whillier A. A fresh look at the performance of cooling towers. *ASHRAE Transactions*. 1976;**82**:269-282
- [12] Agarwal A, Lang J. *Course Materials for 6.002 Circuits and Electronics*. MIT OpenCourseWare (PDF). Boston: Massachusetts Institute of Technology; 2007
- [13] Groppia G, Bellolie A, Tronconi E, Forzatti P. A comparison of lumped and distributed models of monolith catalytic combustors. *Chemical Engineering Science*. 1995;**50**(17):2705-2715
- [14] Ja MK, Koyama S. Numerical and experimental investigations on a two-bed mode adsorption chiller, ICR 2007. Refrigeration creates the future. In: *Proceedings of the 22nd IIR International Congress of Refrigeration*; 21–26 August 2007; Beijing, China
- [15] Ja MK, Choo FH, Li B, Chakraborty A, Dass ETM, Zhao K, et al. Two-dimensional numerical analysis of membrane-based heat and mass cross-flow exchanger. *Heat Transfer Engineering*. 2017;**38**(4):438-445
- [16] Kumja M, Ng KC, Yap C, Yanagi H, Koyama S, Saha BB, et al. Modeling of a novel desorption cycle by dielectric heating. *Modern Physics Letters B*. 2011;**23**(3):425-428
- [17] Kum Ja M. Performance of microwave-activated adsorption cycle: Theory and experiments [Ph.D. thesis]. 2010. Available from: <http://scholarbank.nus.edu.sg/handle/10635/18640>
- [18] Dimitra Psychogiou, Roberto Gómez-García, Raúl Loeches-Sánchez, Dimitrios Peroulis. Hybrid

- acoustic-wave-lumped-element resonators (AWLRs) for high-Q bandpass filters with quasi-elliptic frequency response. *IEEE Transactions on Microwave Theory and Techniques*. JULY 2015; **63**(7):447-449
- [19] 2001 ASHRAE Fundamentals Handbook (SI), Section 5.9. Simultaneous Heat and Mass Transfer Between Water-Wetted Surfaces and Air. Atlanta, GA: ASHRAE; 2001
- [20] ASHRAE Systems and Equipment Handbook (SI). Atlanta, GA: ASHRAE; 2016
- [21] Bird RB, Stewart WE, Lightfoot EN. Transport Phenomena. New York: John Wiley and Sons; 1960
- [22] Incropera FP, DeWitt DP. Fundamentals of Heat and Mass Transfer. 4th ed. New York: John Wiley and Sons; 1996
- [23] Chilton TH, Colburn AP. Mass transfer (absorption) coefficients—Prediction from data on heat transfer and fluid friction. *Industrial and Engineering Chemistry*. 1934;**26**:1183
- [24] Bedingfield GH Jr, Drew TB. Analogy between heat transfer and mass transfer—A psychometric study. *Industrial and Engineering Chemistry*. 1950;**42**:1164
- [25] McElgin J and Wiley DC. Calculation of coil surface areas for air cooling and dehumidification. *Heating, Piping, and Air Conditioning*. March 1940;**12**(3):195
- [26] Kusuda T. Graphical method simplifies determination of air coil, wet heat-transfer surface temperature. *Refrigerating Engineering*. 1957;**65**:41
- [27] 2001 Standard for Forced-Circulation Air-Cooling and Air-Heating Coils, AHRI Standard 410-2001. Arlington, VA: Air-Conditioning, Heating and Refrigeration Institute; 2001
- [28] Schmidt TE. La Production Calorifique des Surfaces Munies d'ailettes, Annexe, Du bulletin De L'Institut International Du Froid, Annexe G-5. 1945
- [29] Brown G. Theory of Moist Air Heat Exchangers. vol. 77. Stockholm, Sweden: Transactions of the Royal Institute of Technology; 1945. pp. 12-15
- [30] Ware CD, Hacha TH. Heat Transfer From Humid Air to Fin and Tube Extended Surface Cooling Coils, ASME Paper No. 60-HT-17. New York, NY, USA: American Society of Mechanical Engineers; 1960
- [31] Cheremisinoff NP, Cheremisinoff PN. Cooling Towers: Selection, Design, and Practice. Ann Arbor, MI: Ann Arbor Science Publishers; 1981
- [32] Nellis G, Klein S. Heat Transfer. Cambridge: Cambridge University Press; 2008